REPORT DOCUMENTATION PAGE

Form Approved
OMB No. 0704-0188

1. AGENCY USE ONLY *(Leave blank)*	2. REPORT DATE	3. REPORT TYPE AND DATES COVERED
	November 2003	Final

4. TITLE AND SUBTITLE
Evaluation of the Microvision Helmet-Mounted Display Technology for Synthetic Vision Application Engineering Prototype for the Virtual Cockpit Optimization Program

5. FUNDING NUMBERS
PE - 622787A
PR - 879
TA - P
WU - DA361539

6. AUTHOR(S)
Thomas H. Harding, J. Steve Martin, Howard H. Beasley, Clarence E. Rash

7. PERFORMING ORGANIZATION NAME(S) AND ADDRESS(ES)
U.S. Army Aeromedical Research Laboratory
P.O. Box 620577
Fort Rucker, AL 36362-0577

8. PERFORMING ORGANIZATION REPORT NUMBER
2004-02

9. SPONSORING / MONITORING AGENCY NAME(S) AND ADDRESS(ES)
U.S. Army Medical Research and Materiel Command
504 Scott Street
Fort Detrick, MD 21702-5012

10. SPONSORING / MONITORING AGENCY REPORT NUMBER

11. SUPPLEMENTARY NOTES

12a. DISTRIBUTION / AVAILABILITY STATEMENT
Approved for public release, distribution unlimited

12b. DISTRIBUTION CODE

13. ABSTRACT *(Maximum 200 words)*
In support of the Virtual Cockpit Optimization Program (VCOP), an image quality evaluation was conducted on the Version #3 prototype of a retinal scanning display helmet-mounted display (HMD). The VCOP HMD is a binocular, full-color display with fully overlapped fields-of-view. Optical measurements included exit pupil characteristics, luminous response and uniformity, modulation and contrast transfer functions, field-of-view (FOV), and see-through transmission. Satisfactory measures of performance were found for exit pupil size and shape, FOV, luminance uniformity and presence of aberrations. Performance and design issues that were found in need of improvement were: (1) system stability following calibration, (2) increased physical eye clearance, (3) spatial filtering of high frequency noise, (4) improved lens coatings to improve see-through light transmission, (5) reduced size of lens/optics, and (6) miniaturization of electronics, if requirements go beyond simulation.

14. SUBJECT TERMS
helmet-mounted display (HMD), Virtual Cockpit Optimization Program (VCOP), image quality, test and evaluation

15. NUMBER OF PAGES
24

16. PRICE CODE

17. SECURITY CLASSIFICATION OF REPORT	18. SECURITY CLASSIFICATION OF THIS PAGE	19. SECURITY CLASSIFICATION OF ABSTRACT	20. LIMITATION OF ABSTRACT
UNCLASSIFIED	UNCLASSIFIED	UNCLASSIFIED	SAR

Table of contents

List of figures

Table of contents (continued)
List of figures (continued)

Table of Contents (continued)
List of figures (continued)

Page

List of tables

Introduction

The Virtual Cockpit Optimization Program (VCOP) focuses on optimizing the workload of the pilot in today's and future advanced military aircraft. The concept of the VCOP is to provide the pilot with information such as sensor imagery, flight data, and battlefield information in a clear and intuitive manner to increase situational awareness, thus making the aircraft easier and safer to fly while also improving mission performance. The VCOP recently completed a simulation demonstration and human factors evaluation of the integrated advanced technologies in a rotorcraft simulator at the Army's Advanced Prototyping, Engineering and Experimentation (APEX) Laboratory at Redstone Arsenal, Alabama. VCOP will continue to utilize simulation to evaluate the effectiveness of the technologies as it progresses towards a flight evaluation.

The majority of the VCOP activity involves the integration of advanced, independently developed technologies into a single system that represents a significant leap ahead in cockpit design philosophies. Rather than concentrating on the aircraft and how it can be retrofitted to meet the needs of the next generation warfighter, VCOP furnishes pilots with the necessary enhanced capabilities to perform their jobs more efficiently. According to the Product Manager for Aircrew Integrated Systems (PM ACIS), VCOP comprises the following six independently developed technologies:

- A full color, high resolution, high brightness helmet-mounted display (HMD) that incorporates retinal scanning display (RSD) technology
- A three dimensional audio system
- A speech recognition system
- A situational awareness tactile vest
- An intelligent information management system
- Crew-aided cognitive decision aids

PM-ACIS tasked the U.S. Army Aeromedical Research Laboratory to evaluate the first technology, the full color HMD. Microvision, Inc., Bothel, Washington, developed the HMD as a demonstration of the application of HMD technology for synthetic vision. This system was comprised of a biocular HMD, a photonics/electronics module, notebook computers for generating the left and right side imagery, and supporting hardware (Figure 1).

Testing of the HMD

Most of the tests were performed using a custom-built HMD tester that accommodated either a monochrome or a color camera and an optometer. A photograph of the tester is shown in Figure 2. The tester provided precise positioning of the test instrument within the field-of-view (FOV) of the HMD. The HMD's exit pupil was co-located with the center of rotation of the test instruments (Figure 3). From precision potentiometers, signals were generated that provided exact readout (in degrees) of the center position of

the test instrument relative to the HMD's FOV. The zero position (0,0) coincided with the position of the center pixel (640, 512) of the 1280 x 1024 display.

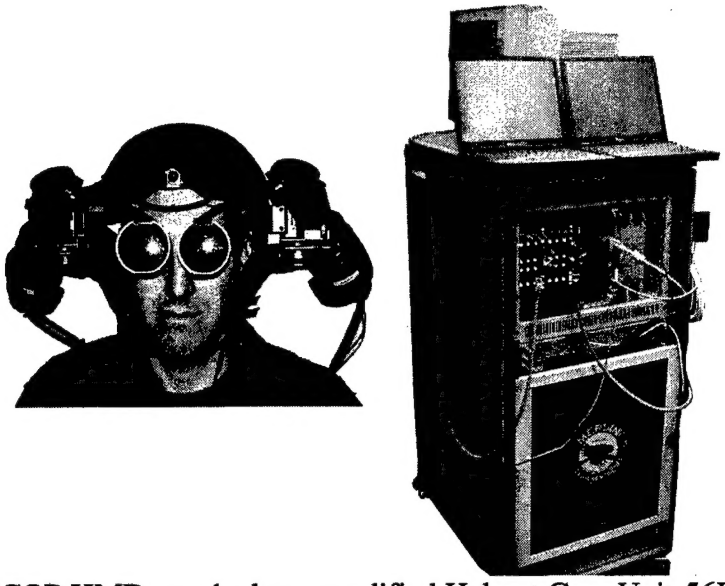

Figure 1. The VCOP HMD attached to a modified Helmet Gear Unit-56P (HGU-56P) helmet without the typical ear cups and with much of the foam insert missing (left). The photonics/electronics rack mount system and supporting computers are shown on the right. The laptops controlled imagery displayed on each side of the HMD. The computer monitor shown in the rear was part of a computer system that controlled the photonics unit itself.

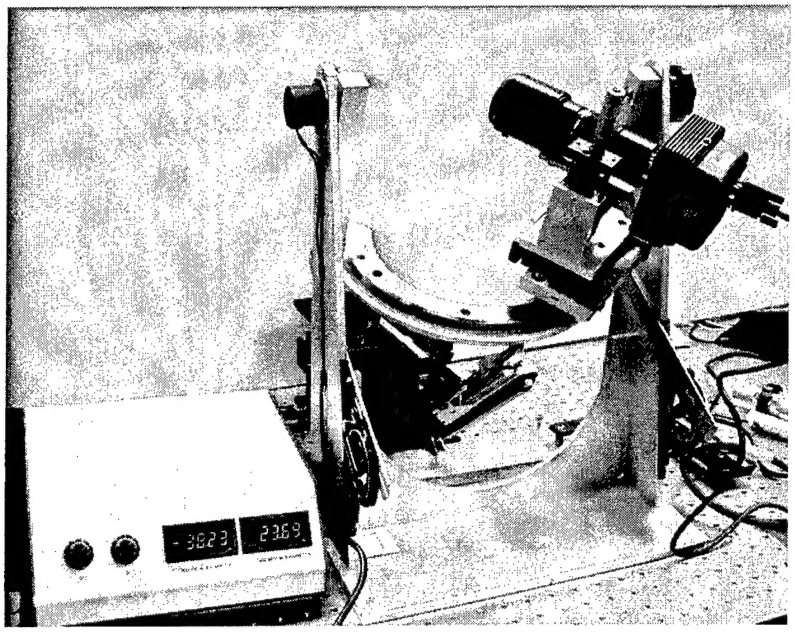

Figure 2. Custom built HMD tester with monochrome camera. Position readout, in degrees, was provided by precision potentiometers attached to the positioner.

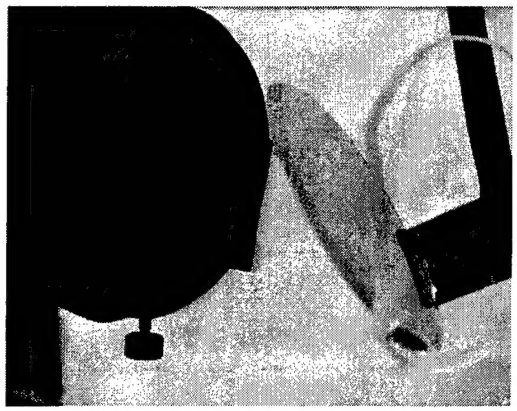

Figure 3. HMD exit pupil positioned and focused onto a 5-millimeter (mm) iris mounted to the front of the test instrument. The middle of the 5-mm iris was aligned with the center of rotation of the test system. This photograph was taken during an earlier evaluation of the Microvision's Aircrew Integrated Helmet System HMD.

Most of the measurements in this analysis were made with either a monochrome or color digital camera. The cameras (DVC-1310s) were interfaced to the computer via the IEEE 1394 protocol. The progressive scan cameras had a horizontal resolution of 1300 by a vertical resolution of 1030 pixels with 10 bits per pixel. The color camera used a Bayer Color Filter Array (CFA) pattern composed of two green, one red, and one blue pixel in every four by four pixel square. The relative sensitivity of this camera is shown in Figure 4. The color camera was not used for critical spatial resolution measurements.

With the camera's telephoto lens focused to infinity, captured images had an approximate 9.54 to 1 ratio of imaged pixels to an HMD pixel. This ratio, which is very close to the sampling ratio of 10 to 1 recommended for such analyses, was sufficiently high to provide good measures of spatial resolution. The cameras, as well as all other test instruments, were equipped with a 5-mm iris. To determine the scale factor needed to adjust luminance measurements to correct for the iris, two identical Pritchard photometers were taken outside and set side by side. While focusing to infinity and aiming both photometers to the same patch of clear sky, the 5-mm iris was placed over one photometer, and the two luminance-readings were recorded. By calculating ratios, scale factors were determined for the iris. The series was then repeated for the second photometer. In general, however, we only report relative luminance readings, unless it is important that the absolute luminance reading be known.

The monochrome camera was equipped with a cooling device that reduced the camera's dark noise. For spatial measurements reference, images were captured with the camera lens cap in place, thus providing a measure of the dark noise. The dark images were processed the same as the real images, and the average dark noise was subtracted from the averaged real image. See the modulation transfer function (MTF) section below for a discussion of the averaging technique.

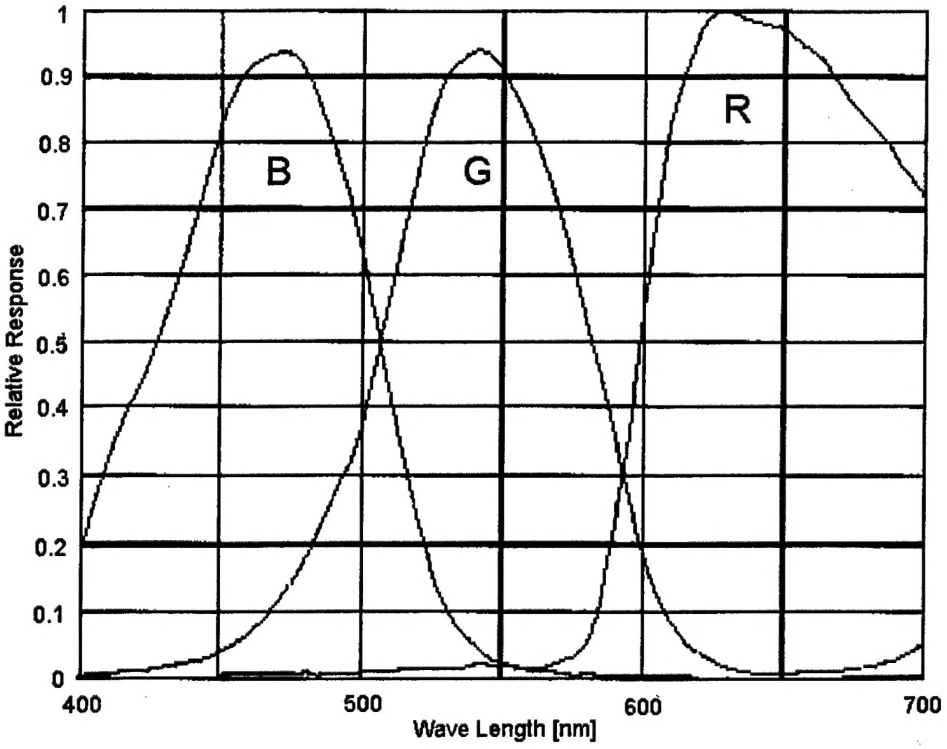

Figure 4. DVC color camera's spectral response.

Exit pupil size and shape

Test equipment: A Sony Mavica digital camera, monitor, computer, millimeter rule, and Matrox Image Inspector version 4.0 software.

Test procedure: A grid pattern was displayed on the HMD with the center pixel clearly indicated. The camera was focused to infinity and aligned with the center pixel of the left or right display. Proper alignment required the center pixel to be in the middle of the monitor with best focus over the entire monitor image. Once proper alignment was achieved, the camera was refocused on the exit pupil, and the HMD alignment image was replaced with a uniform field with each pixel set to maximum drive levels (255, 255, 255). This image filled the exit pupil with light, and the image of the exit pupil was stored for later analysis. A millimeter rule was co-located with the position of the exit pupil, and a photograph was taken again. This photograph provided the basis for measuring the size of the exit pupil. Approximate uniformity within the exit pupil was assessed by evaluating the photographic image.

Results: Figure 5 shows the exit pupil captured from the left side. The hexagonal exit pupil was approximately 17 mm wide by 14 mm high. A color separation was noted in the exit pupil. This color separation was visible in the original. Figure 5 also shows a profile of a scan of the horizontal meridian of the photographic image.

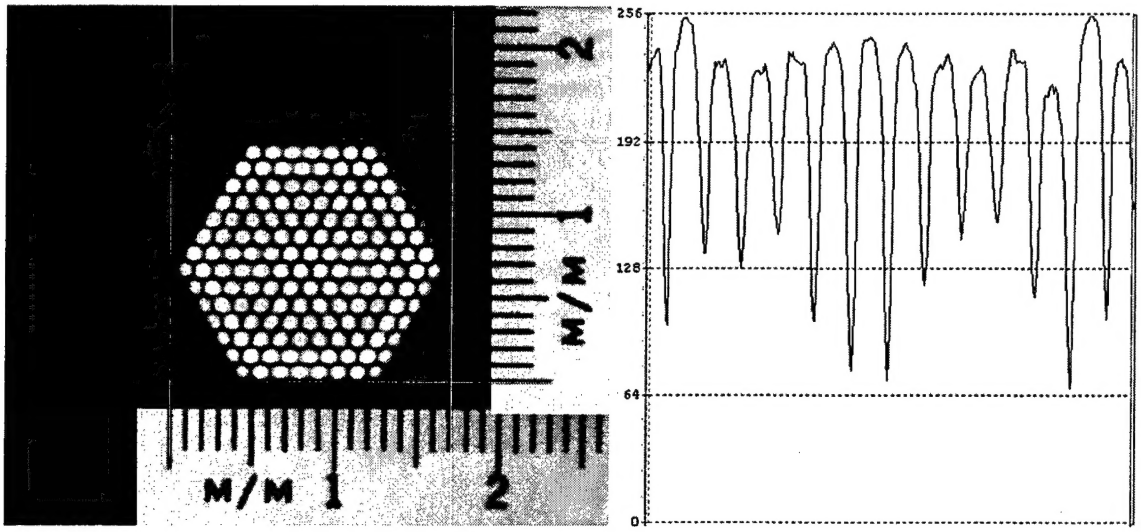

Figure 5. Exit pupil with millimeter rules. The horizontal rule was photographically copied, transformed, and pasted to form the vertical rule. Faint horizontal and vertical lines show where the size measurements were taken. The graph on the left shows a line profile through the horizontal meridian of the exit pupil after the image was converted to a grayscale image.

Eye relief

Test equipment: Rear projection screen, Sony Mavica digital camera, and positioning system.

Test procedure: A rear projection screen was used to locate the exit pupil position. This was accomplished by moving the rear projection screen along the optical axis until best focus was achieved (Figure 6). Eye relief can be expressed as either physical eye relief or optical eye relief. Physical eye relief (eye clearance distance) is defined, for the purpose of this report, to be the straight-line distance from the cornea (positioned at the exit pupil) to the vertical plane defined by the first encountered physical structure of the system. Optical eye relief is the straight-line distance from the cornea to the last optical element of the HMD system. In most cases, physical eye relief is much less than optical eye relief and is more relevant in addressing compatibility with ancillary equipment, i.e., gas mask, oxygen mask, spectacles, etc. (Rash et al., 2002). Once the rear projection screen was placed at the exit pupil, a camera mounted on the right was moved parallel to the optical axis until the camera angle was orthogonal to the optical axis of the HMD and lateral to the position of the rear projection screen and combiner lenses. From this position, a photograph was taken of the rear projection screen and the HMD's combiner lenses. By placing a millimeter rule under the rear projection screen, the physical eye relief could be determined (Figure 7).

Results: From Figure 7, eye relief can be determined. Physical eye relief is characterized by the linear distance from line A (coincident with the exit pupil as marked by the rear projection screen) to line B. Optical eye relief is characterized by the linear distance from line A to line C, which is coincident with the center of the lens. Physical eye relief was measured as 9.25 mm, and optical eye relief was measured as 29 mm.

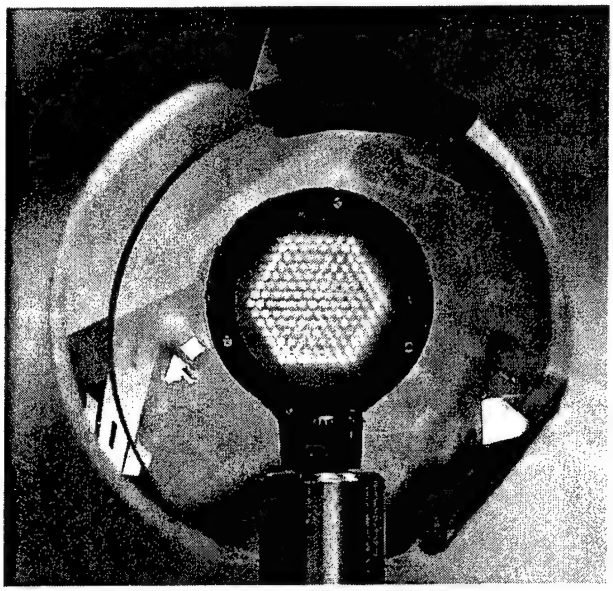

Figure 6. Exit pupil focused onto a rear projection screen sandwiched between a circular clamp. The screen was moved fore and aft until best focus was achieved.

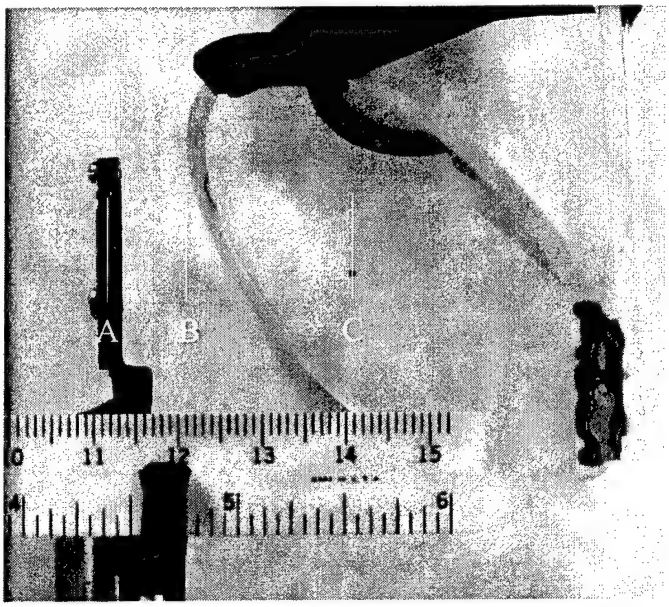

Figure 7. Physical and optical eye relief measurements. Optical eye relief is the linear distance from line A to C. Physical eye relief is the distance from A to B.

Field-of-view

Test equipment: HMD tester with charge-coupled device (CCD) camera, computer, and a computer image that clearly marks extreme positions of the FOV.

Test procedure: FOV was measured by positioning the CCD camera along either the rotational or elevational axis of the HMD tester until the extremes of the FOV become visible. The camera was then moved until the limits of the FOV were centered upon a reference point. The reference point, in our case, was a mouse cursor placed in the middle of the image as seen in the computer monitor. The limits of the vertical and horizontal FOVs were noted and the angular distances calculated.

Results: The results are shown in Table 1.

Table 1.
Field-of-view results (in degrees).

	Left side	Right side
Horizontal FOV	41.68	41.55
Vertical FOV	33.17	33.52

See-through transmission

Test equipment: A Gamma Scientific RS-12 standard tungsten lamp, a Photo Research PR704 Spectrascan,™ and a computer.

Test procedure: The RS-12 standard lamp was placed in front of the left optical lens assembly, with the lamp surface orthogonal to the optical axis. With the lens assembly retracted (down position), a spectral scan of the lamp was performed and stored on the computer. The lens assembly then was placed in position to intersect the lamp, and the spectral scan was repeated. The second scan then was divided by the first scan to find the attenuation in light due to the HMD optics. These data then were plotted as a transmissivity curve. This procedure then was repeated for the right channel.

Results: The results are presented in Figure 8. The average transmittance was approximately 9.24 percent (%).

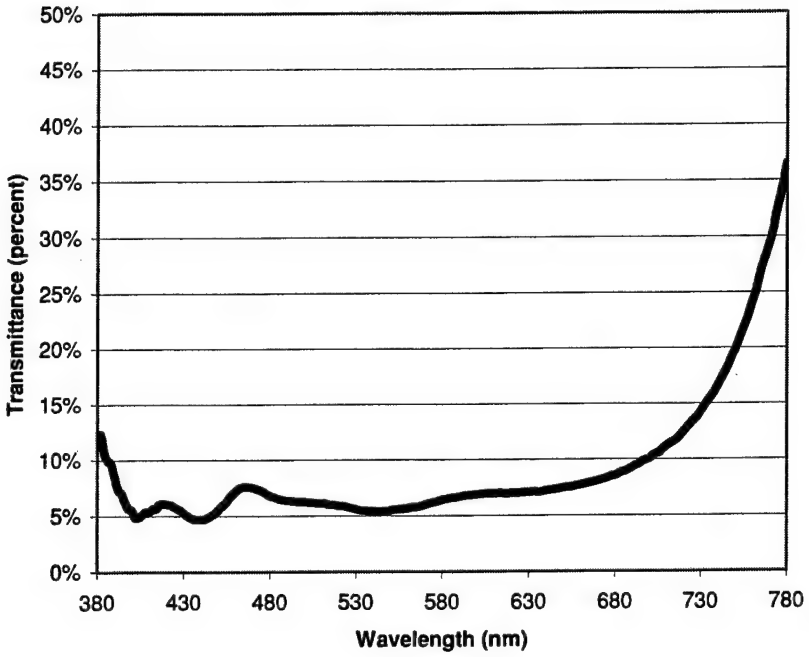

Figure 8. See-through transmittance of the left-side optics

Spectral output

Test equipment: Photo Research PR704 Spectrascan.™

Test procedure: The spectral distribution of the light output from the HMD was measured using a Photo Research PR704 Spectrascan.™ The PR704 provided a fast and highly repeatable scan. A test image was presented to the right side channel where all pixels were set to a maximum level (255, 255, 255). The Spectrascan™ was focused on the middle of the HMD's FOV, and the scans were taken with the largest aperture (a rectangular aperture measuring 1.5 degrees by 0.5 degree).

Results: Figure 9 shows the three monochromatic peaks corresponding to the red, green and blue lasers. The red laser peaked at 638 nm, the green laser peaked at 532 nm, and the blue laser peaked at 458 nm. On the day previous to the day these measurements were made, the three lasers were calibrated to provide equal luminance.

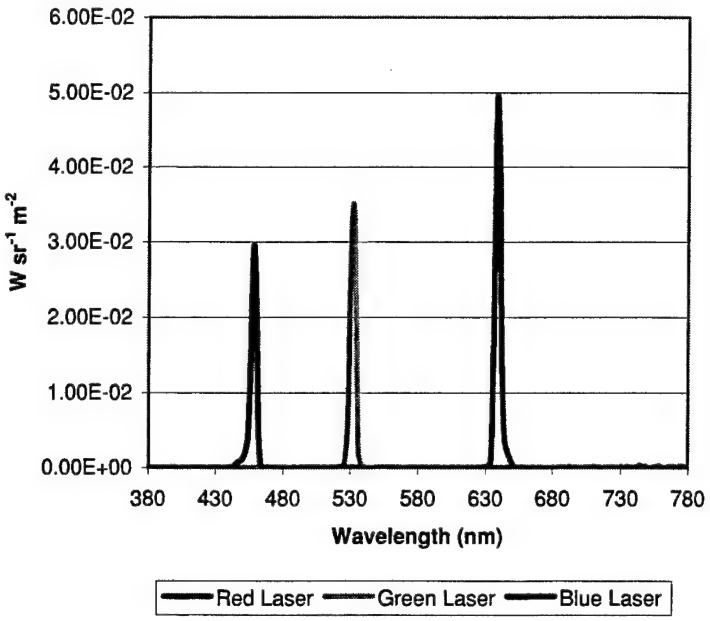

Figure 9. Spectral output of the HMD's right channel.

Aberrations

Test equipment: The HMD tester fitted with a dioptometer with a 5-mm iris.

Test procedure: An image of a grid pattern consisting of vertical and horizontal lines was presented to the left side of the HMD. The dioptometer, with a 5-mm artificial pupil, was placed at the exit pupil. An observer viewed the grid pattern with the dioptometer and focused first on the vertical lines and then on the horizontal lines. Recordings of the dioptometer's settings were made for each focus adjustment. Field curvature, spherical and astigmatic aberrations were measured. Field curvature was measured by horizontal or vertical rotation through the vertical and horizontal meridians of the FOV. Spherical aberration was measured as a function of decentration. The difference between the vertical and horizontal focus provided an estimate of spherical aberration or astigmatic error.

Results: Aberrations were generally near zero and never exceeded ∀0.375 diopters (Figures 10 and 11).

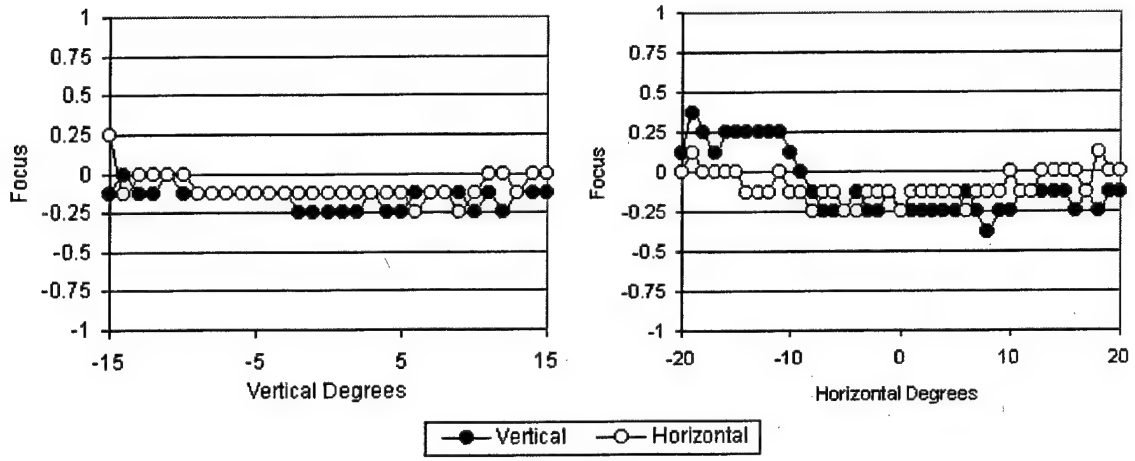

Figure 10. Field of curvature of the left oculars for the vertical and horizontal meridians.

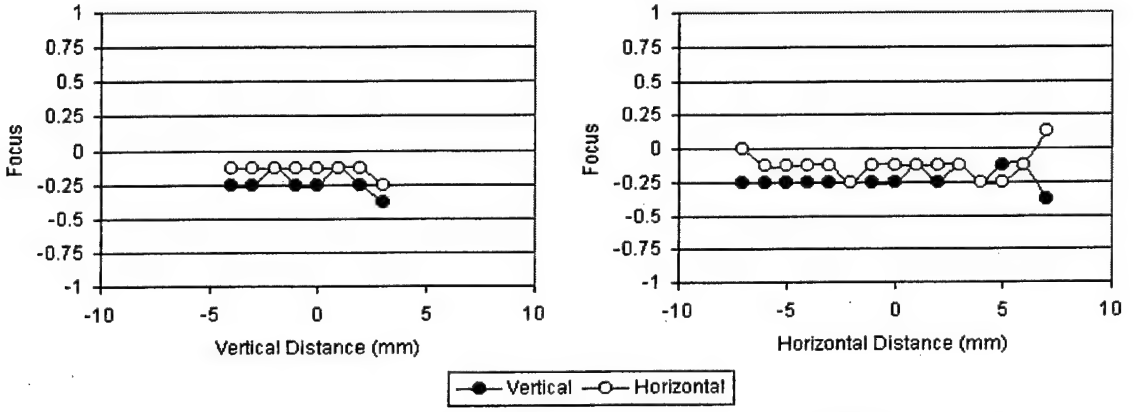

Figure 11. Optical aberration as a function of decentration (in millimeters). The differences between the vertical and horizontal focus is an estimate of astigmatic error.

Luminance response

Test equipment: Model 1980A Prichard photometer with a 5-mm iris.

Test procedure: To measure the system's Gamma, a 40-pixel square target in the middle of the display was set to a level of 0 to 255 for each of the colors, in increments of 8. The photometer was focused to infinity and aligned with the middle of the square. A reading was made for each of the color settings. This procedure was repeated for a gray scale pattern where all three colors were set to the same value for each increment. In this condition, photometric readings were made for each increment level from 0 to 255.

Results: Results are shown in Figures 12 and 13. The red, green, and blue laser data were at different luminance levels, even though the luminance from the three lasers was calibrated the previous day. To see distinctions between response dynamics, the red

green and blue data were normalized to their maximum values in Figure 13. The green curve shows a more accelerated response characteristic.

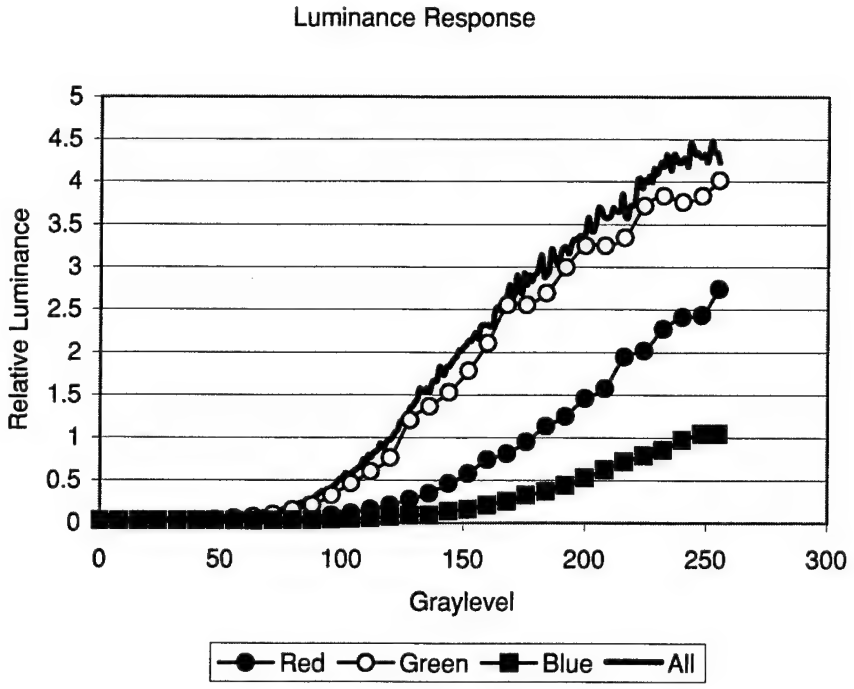

Figure 12. Luminance responses for the red, green and blue lasers and for the composite (all lasers on).

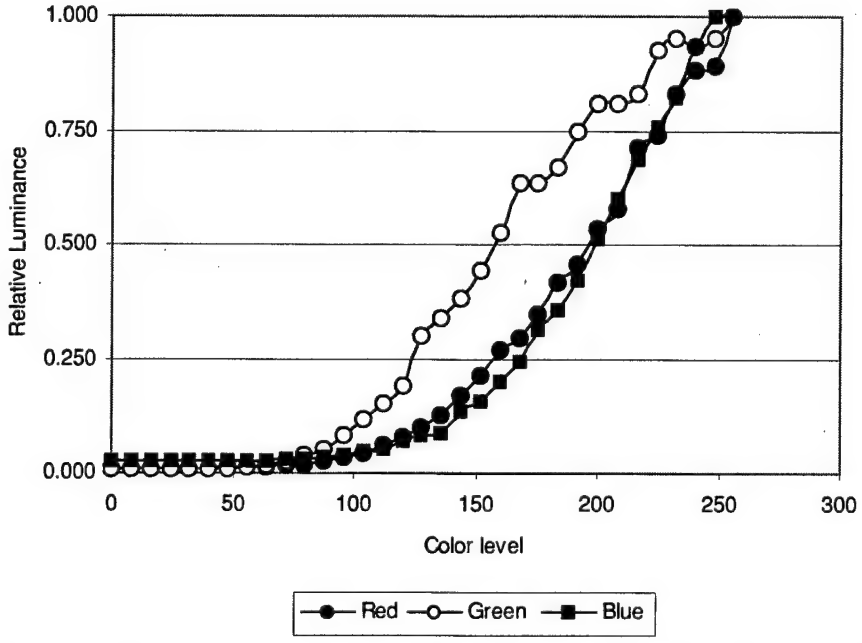

Figure 13. Relative luminance responses for the red, green, and blue laser data shown in Figure 12. All data were normalized to their maximum values.

Luminance uniformity

Test equipment: CCD monochrome camera with a telephoto lens, HMD tester, computer, and Matrox Image Inspector software.

Test procedure: Luminance was measured as a function of FOV position. A 25-square pattern (each square 80 by 60 pixels with color values of 255, 255, 255) was presented with the background set to zero (0, 0, 0). The squares were distributed over the FOV according to the scheme shown below. A 1280 by 1024 pixel image was displayed where the center pixels of the squares were positioned at the 10%, 30%, 50%, 70% or 90% positions. For example, the center pixel of the top left square was positioned at coordinates (128,102), where the top-left corner coincides to coordinates (0,0). The (128,102) position corresponds to the 10% lateral and the 10% down position. The display was imaged by a CCD camera with a telephoto lens and captured on computer; each square was imaged separately. The relative luminance was measured using the image software.

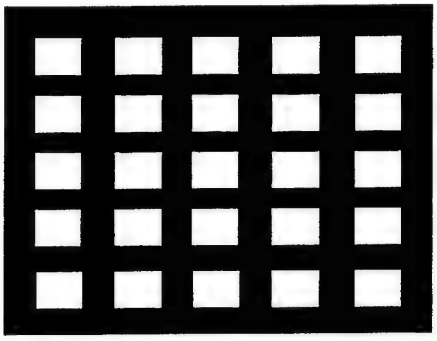

Results: The luminance uniformity results are presented in Table 2 and are graphically presented in Figure 14. The measurements are given as a % deviation from the mean luminance. Note that most squares are within ± 20%, with the exception of the lower right corner, which is higher, and the middle, which is lower.

Table 2.
Luminance uniformity results - deviation from the average luminance.

7.67%	-4.77%	-9.28%	4.58%	-4.46%
0.46%	-4.66%	-22.53%	-14.50%	21.84%
13.45%	0.02%	-22.87%	-14.03%	17.54%
6.21%	-10.11%	-27.18%	20.92%	11.50%
4.34%	6.34%	-16.04%	8.66%	26.91%

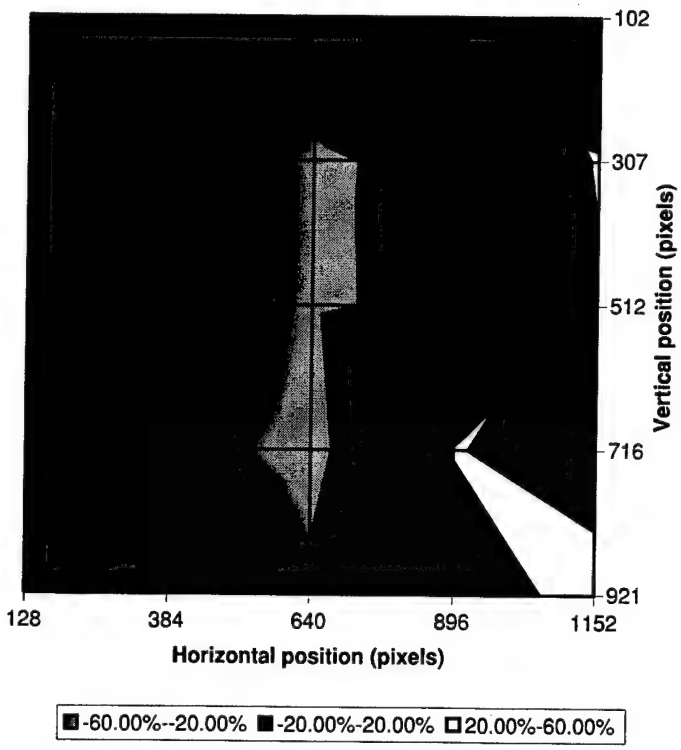

Figure 14. Luminance uniformity as a function of FOV position. Most of the display was within ∀20% of the average luminance (-20% to 20% condition) red area. Note: The "-" symbol also represents the word "to" in the legend.

Contrast and contrast uniformity

Test equipment: CCD monochrome camera with a telephoto lens, HMD tester, computer, and Matrox Image Inspector software.

Test procedure: Contrast was measured as a function of FOV position. Contrast/contrast uniformity was measured using the same 25-bright-square pattern as shown above (Luminance uniformity section). Images of all of the squares were captured by computer, and the resulting images were analyzed. Contrast ratios were measured by methods evaluating the middle of each of the 25 squares and a dark area of 80 HMD pixels to the right of each square. A region-of-interest was selected in the middle of each bright square (an area of 64 by 64 photographic pixels) and within the darkened area. The average intensity was computed for each position. Contrast ratios were calculated by dividing the peak luminance by the background luminance.

Results: Table 3 shows the contrast values for each of the 25 squares. The average contrast ratio was 32.78. Table 4 and Figure 15 show the deviation from the average contrast. Note that the largest deviation from the mean was in the lower right corner, where the contrast was 35.59% higher than the average.

Table 3.

Contrast and contrast uniformity results - contrast ratios calculated from the twenty-five squares.

35.61	31.80	30.47	36.83	24.27
36.57	30.85	24.86	29.85	41.92
34.21	30.54	26.69	28.20	33.18
32.35	28.62	25.80	39.88	37.93
35.09	37.56	28.56	33.18	44.43

Table 4.

Contrast and contrast uniformity results - deviations from the average contrast ratio.

8.66%	-2.95%	-7.02%	12.39%	-25.94%
11.59%	-5.87%	-24.13%	-8.92%	27.93%
4.38%	-6.80%	-18.55%	-13.95%	1.24%
-1.28%	-12.66%	-21.28%	21.70%	15.74%
7.09%	14.62%	-12.84%	1.25%	35.59%

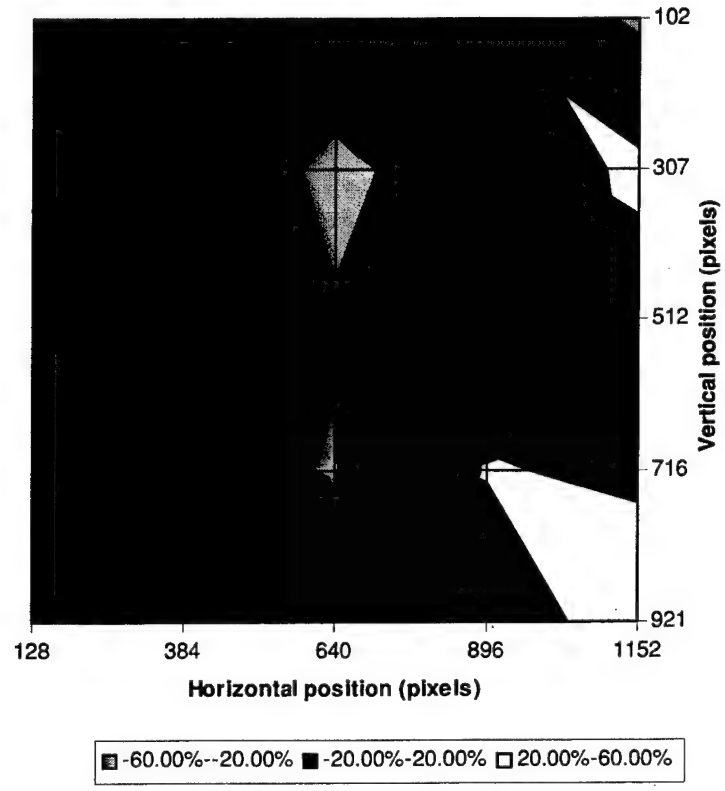

Figure 15. Average deviation from the mean contrast (from Table 4) as a function of FOV position. This graph is very similar to the luminance uniformity graph shown in Figure 14.

Modulation transfer function

Test equipment: Monochrome digital camera with a telephoto lens and 5-mm iris, computer, Matrox Image Inspector version 4 software, and Fast Fourier Transform (FFT) software.

Test procedure: The monochrome digital camera imaged a single vertical or horizontal line in the middle of the display; the image captured and stored on a computer for analysis. In addition, an equal-size image, taken with the lens cap on, was collected to determine the amount of dark noise. Image magnification was 9.54 to 1 (number of pixels in the captured image for each one pixel in the display). To obtain a line spread function, a region-of-interest of 100 by 512 was collected in the middle of the image and averaged to yield an array of 1 by 512. A one-dimensional FFT was performed on the averaged data, and the MTF was calculated. Care was taken to assure that the vertical or horizontal line was properly aligned with the region-of-interest so as not to contaminate the results.

Results: Figure 16 shows the vertical and horizontal MTFs collected from the right channel. For the right channel FOV of 41.55° by 33.17° and the 1280 by 1024 pixel format, an average Nyquist frequency of 15.42 cycles/degree was determined. At this Nyquist frequency, the vertical MTF produced a modulation of 0.425 and a modulation of 0.173 for the horizontal MTF. The discrepancy between the two curves is somewhat understandable when you consider the vertical MTF is obtained from a single horizontal scan line. On the other hand, the horizontal MTF is derived from a vertical line made up of many pixels that must be turned on and off accurately during the scan.

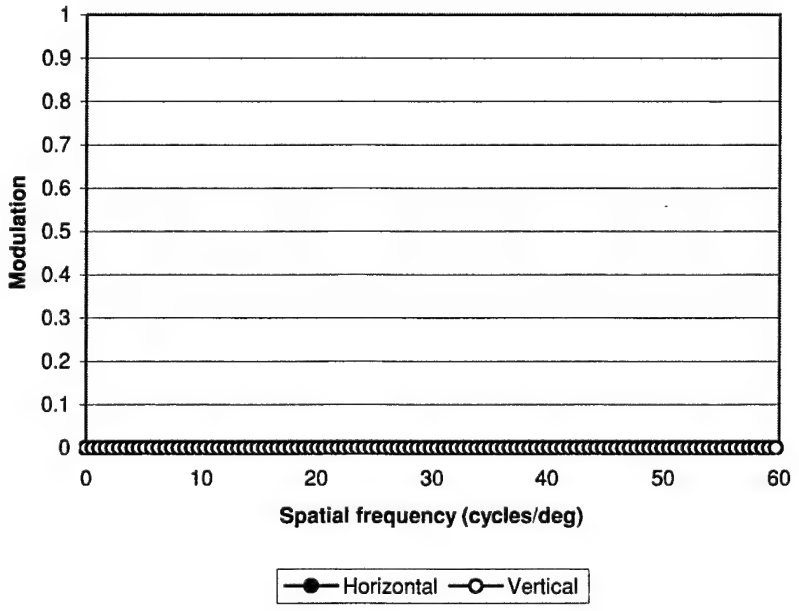

Figure 16. Vertical and horizontal MTFs from the middle of the right channel's FOV.

Much of the discrepancy between the horizontal and vertical MTF can be observed by careful consideration of the vertical line and its subsequent profile. The present HMD writes images by scanning four horizontal lines simultaneously. During the retrace, the lines are turned off. To properly calibrate the HMD's imagery, the four lines must be evenly spaced. The line spacing is effectively smaller than the hardware allows, and thus, the pixels on sequential horizontal lines are offset. It is this offset that negates using a point-spread function to define the spatial resolution of this device. The dimensionality requirement of the point-spread function would be violated, since a vertical line cannot be defined by multiple X-coordinates. A point-spread function derived from such a system would still provide an accurate vertical MTF (a curve defined by frequency vectors with $u = 0$). The magnitude of all other frequencies would be invalid. Figure 17 shows the relationship between pixels in four vertical line segments. Figure 18 shows the line profiles collected for horizontal versus vertical line segments.

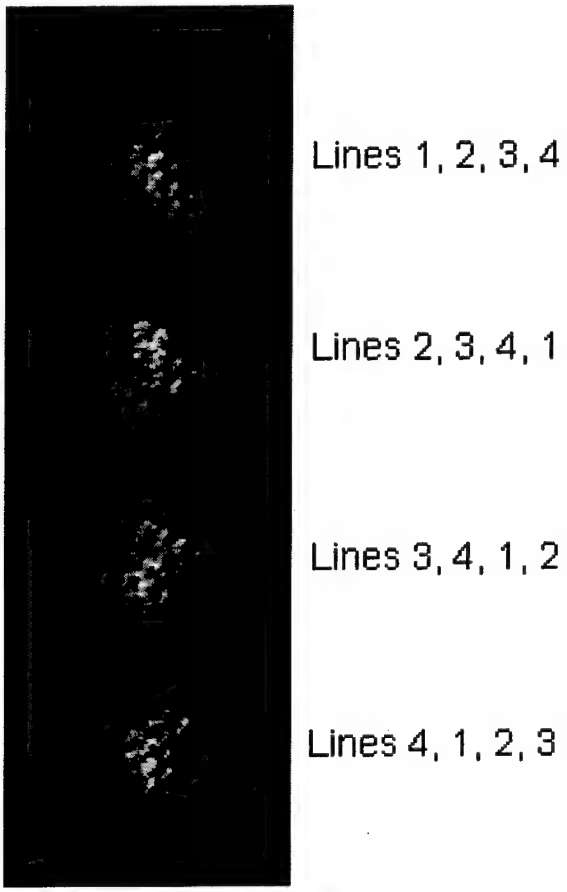

Figure 17. Images of four vertical line segments constructed of four pixels. By numbering the four scanned lines as 1, 2, 3, and 4, the above photograph is enlightening. The top line segment is made up of pixels from lines 1, 2, 3, and 4. Note the obvious skew of the top segment and all subsequent segments.

The MTFs shown in Figure 16 were calculated from the line spreads shown in Figure 18. The vertical line spread is about 50% wider than the horizontal spread due to the skewed relationship between the columns of pixels. At half amplitude, the vertical line spread has a width of about 0.39 degree, compared to 0.26 degree for the horizontal line-spread.

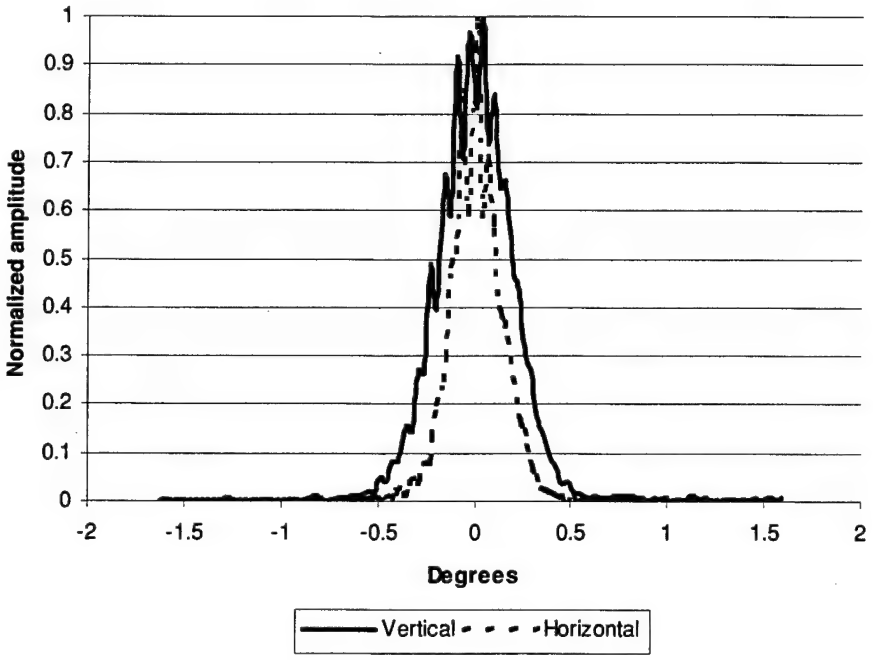

Figure 18. Horizontal and vertical line-spread functions derived from photographic data from the right channel.

Contrast transfer function (CTF)

Test equipment: Monochrome digital camera with a telephoto lens and 5-mm iris, computer, FFT software and Matrox Image Inspector version 4 software.

Test procedure: Grill patterns (vertical and horizontal square wave gratings) of increasing spatial frequency were presented to the right channel in order to measure the CTF. The grill patterns were imaged by the monochrome digital camera and captured by computer. The magnification was approximately 9.54 to 1. Six grill patterns were used (32-on/32-off, 16-on/16-off, 8-on/8-off, 4-on/4-off, 2-on/2-off, and 1-on/1-off). The numbers relate to rows or columns. Thus the 1-on/1-off grill would have a spatial period of 2. These grill patterns related to fundamental spatial frequencies of 0.48, 0.96, 1.92, 3.85, 7.71 and 15.42 cycles/deg.

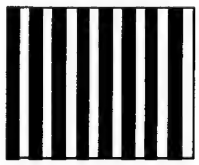

Results: The sample photograph in Figure 19 is a captured image of the horizontal 4-on/4-off grill pattern. Note the pattern of dots/pixels making up the horizontal lines. The spacing of these dots when Fourier transformed have their largest frequency amplitude at 40 cycles/deg (see Artifact section below). To calculate the CTF, two methods were used; each provided similar results. The first method was to average the peaks and troughs from the grating image. This was achieved by sampling from a region-of-interest in the middle of the image/FOV. A 512 by 100 pixel region of interest was selected. An X-profile was obtained by collapsing the data, resulting in a 512 by 1 pixel array. The peaks and troughs in the array were then averaged, and the contrast was calculated based on the Michaelson formula $((L_{max} - L_{min}) / (L_{max} + L_{min}))$. Horizontal and vertical CTFs calculated by this method are shown in Figure 20. The second method was to evaluate the same 512 by 1 pixel array by calculating the standard deviation and then dividing by the mean of the array (Harding et al., 2002). The horizontal and vertical CTFs calculated this way are shown in Figure 21.

Note the similarities between the two sets of curves. The data agree fairly well but the data are not in agreement with the MTF data that show a clear advantage for horizontally aligned patterns. One problem with the CTFs shown in Figure 21 is the vertical CTF at the lowest spatial frequency where the standard deviation was larger than the mean resulting in over a 100% value. This is the result of our data collection procedure. For all of the data, photographs were obtained with a telephoto lens set to maximum magnification. For low frequencies, fewer cycles of the grill pattern were sampled. For the lowest frequency, less than one spatial period was sampled, and this could have caused the errant point.

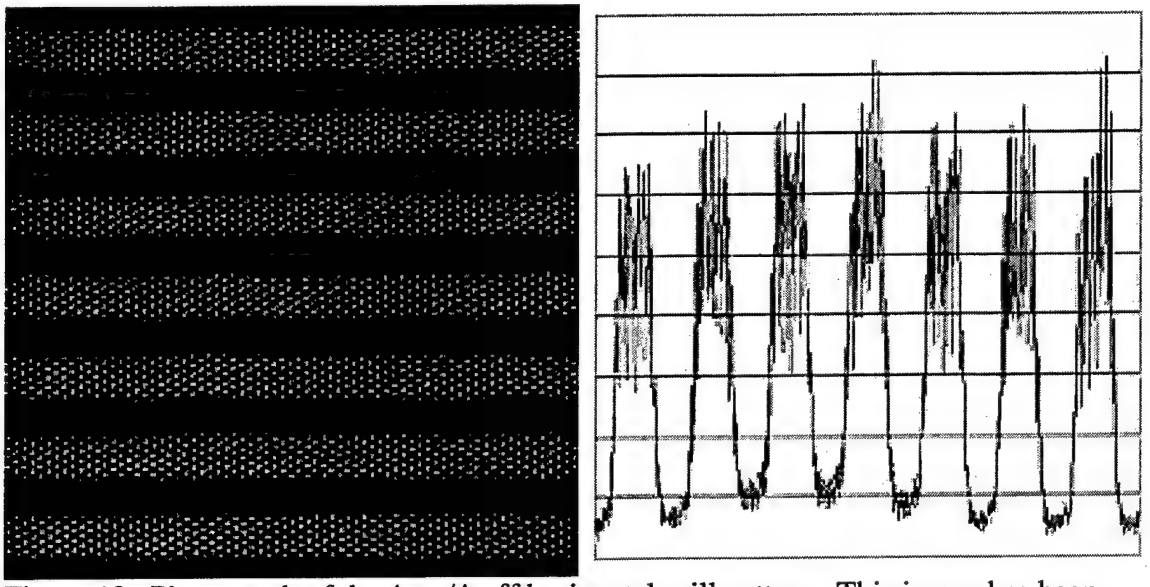

Figure 19. Photograph of the 4-on/4-off horizontal grill pattern. This image has been photographically enhanced for presentation purposes. The curve on the right is the 512-point array taken from the collapsed data (averaged). The noisy peaks are the result of the summed and spatially aligned pixels/dots.

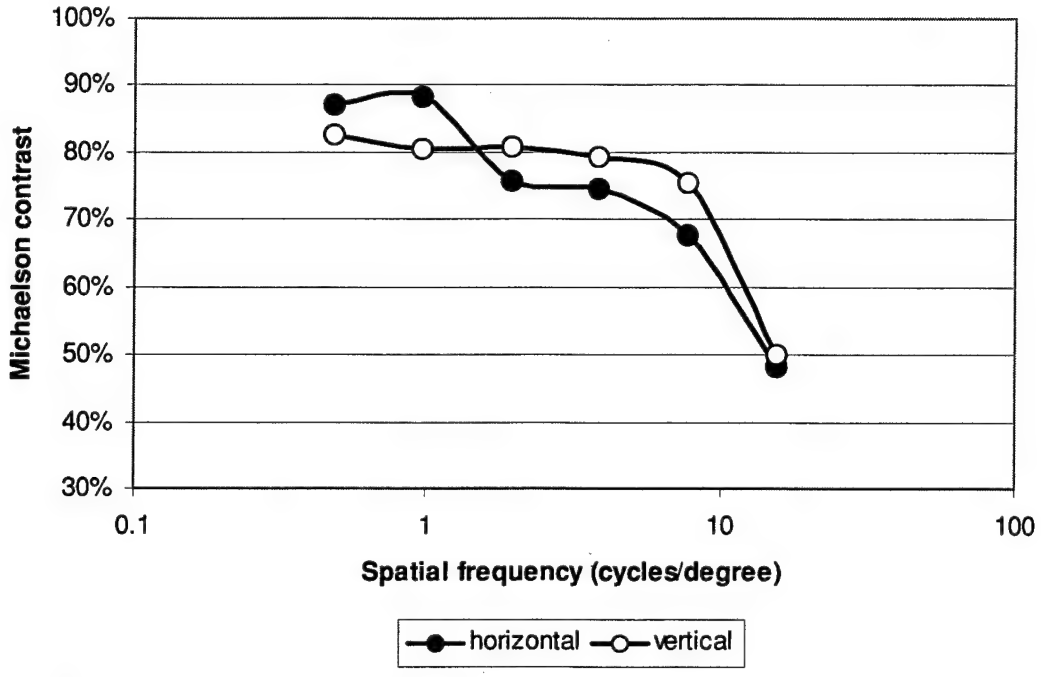

Figure 20. Horizontal and vertical CTFs calculated from the averaged peaks and troughs.

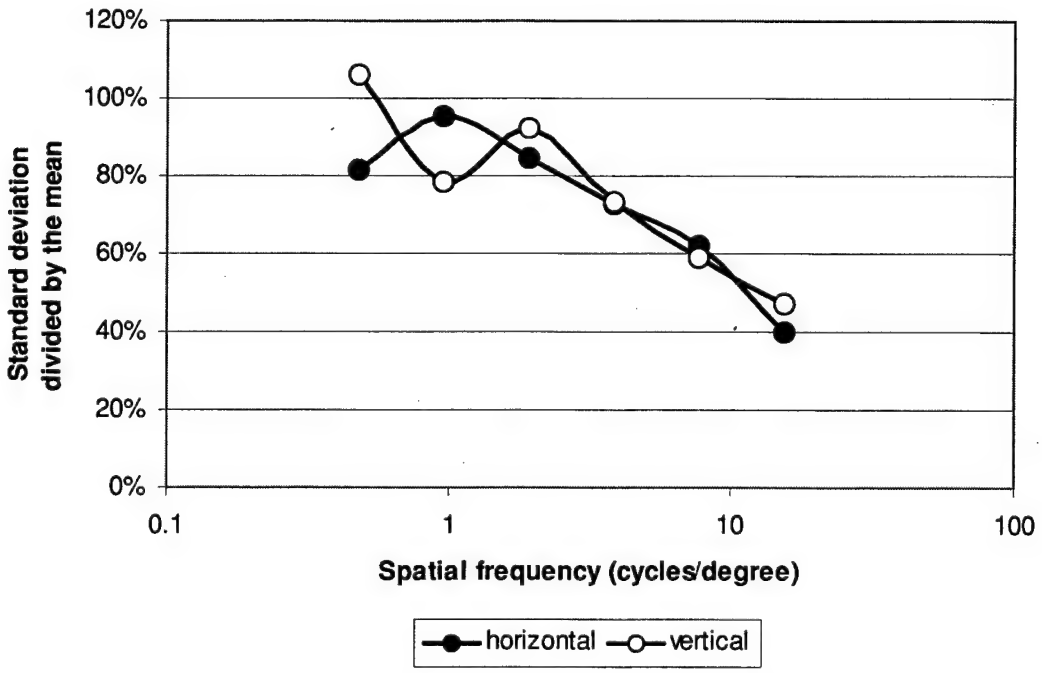

Figure 21. CTFs calculated as the standard deviation divided by the mean.

Artifact

As mentioned above in discussion of Figure 19, photographic data of certain spatial patterns produced a large artifact (or noise factor) centered at about 40 cycles per degree. Figure 22 shows the amplitude spectra of six of the 512-point arrays used to calculate CTFs. Note that each curve peaks near its fundamental frequency and at 40 cycles/degree. Figure 23 shows a noise plot obtained by collapsing the CTF data along the orthogonal axis. The origin of this artifact could be due to the method in which the exit pupil expansion is created. Since the artifact is 2.5 times higher than the Nyquist pattern, it is unlikely to affect the visibility of patterns presented. Psychophysical evidence supports the notion that masking and/or adaptation only affects the detection of spatial frequencies that are within an approximate one-octave bandwidth of the masking or adapting frequency. Thus, the detection of high spatial frequency targets up to the Nyquist frequency should not be affected. However, that is not the case for see-through imagery. Over most of the photopic range of vision, young aviators can see spatial frequency targets approaching 60 cycles/degree (Harding, unpublished results). Thus, the 40-cycles/degree noise could affect the detection of multiple high frequency targets (small targets or detail in larger targets). Figure 24 shows the possible masking affect of the 40-cycles/degree noise. Masking is greatest at 40 cycles/degree and falls-off exponentially from there.

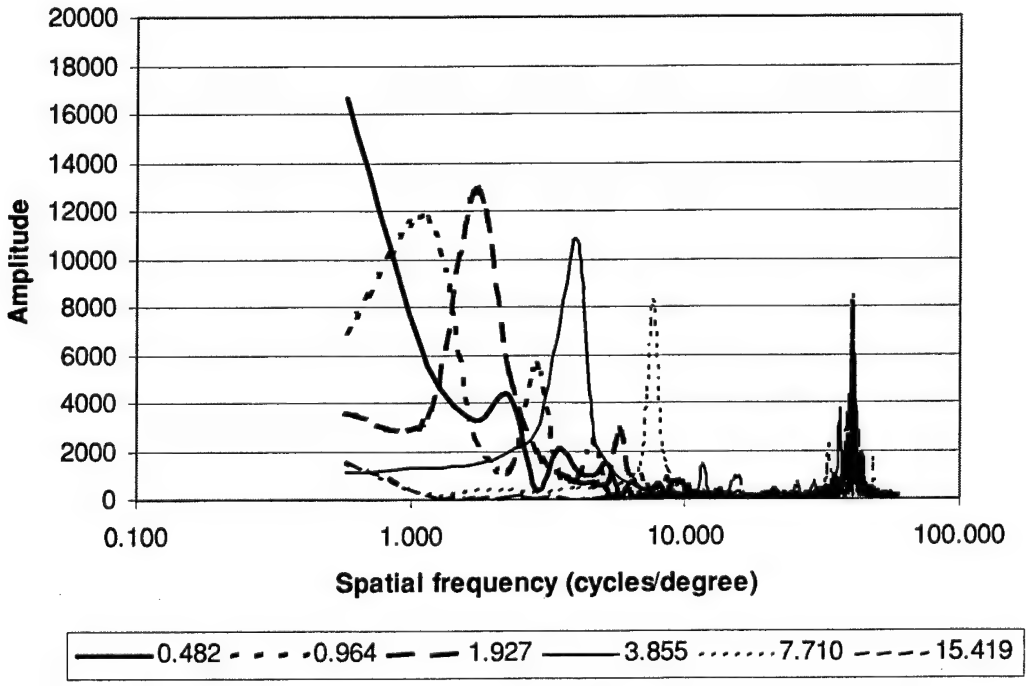

Figure 22. Frequency spectra calculated from the vertical CTF arrays.

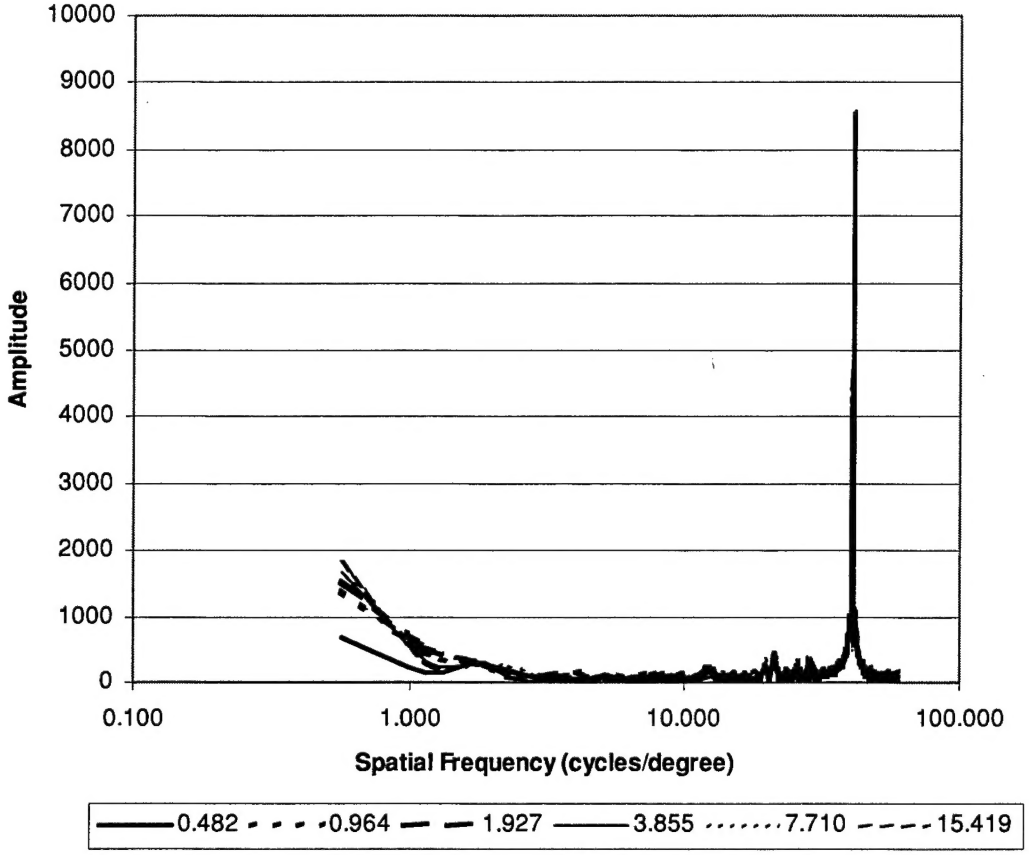

Figure 23. Noise spectra calculated from the horizontal CTF arrays.

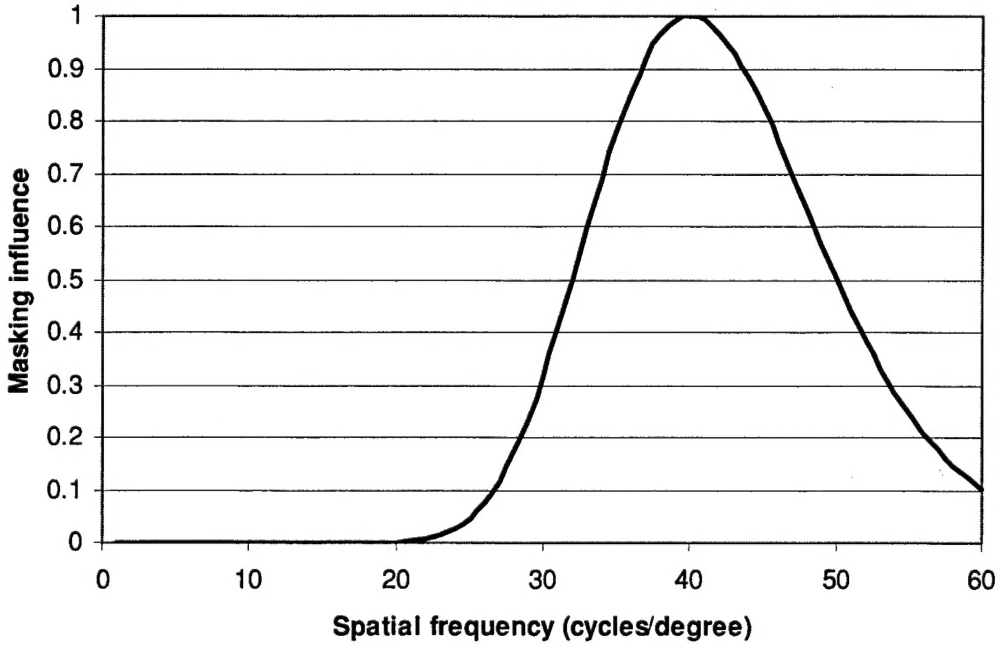

Figure 24. Masking affect of the 40-cycles/degree noise.

Discussion

The Microvision VCOP HMD is a binocular, full-color display with fully overlapping FOVs. The data reported here culminated from an approximate two-week testing period while the system was onsite at the U.S. Army Aeromedical Research Laboratory, Fort Rucker, Alabama. Throughout the testing period, Microvision engineers provided support and assistance. The lasers were adjusted to provide 50 footlamberts at the eye.

The problems encountered during testing were mainly associated with HMD calibration. The four lasers had to be properly aligned. Photometric calibration was performed on the first day. But, by the second day, our tests indicated that the system was again out-of-calibration. The two critical problems encountered were the poor physical eye relief and the 40-cycles/degree noise that could greatly affect high spatial frequency see-through imagery.

The CTF and MTF did not completely agree. This lack of agreement was due mostly to the need to identify or develop better methods of evaluating CTFs for these newer technology display formats. Signal-to-noise ratios may provide an improved metric over current methods (Harding et al., 2001). A view of the text images in Figure 25 show that the small 5 by 5 letters are difficult to decipher, further suggesting that improved metrics are required.

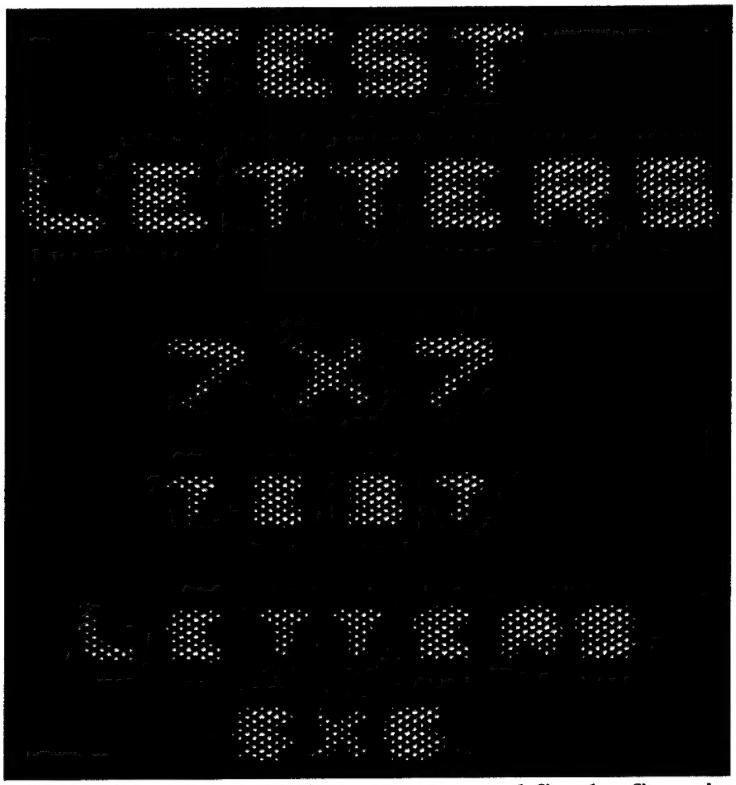

Figure 25. Seven by seven-pixel letters on top and five by five-pixel letters on the bottom. Letters were displayed in the middle of the right-side FOV.

Conclusions

The Microvision VCOP HMD is a complex and sophisticated engineering achievement characterized by good tri-color imagery and adequate resolution, when properly calibrated. Satisfactory measures of performance were found for exit pupil size and shape, FOV, luminance uniformity and presence of aberrations. Performance and design issues that could be improved upon are: (1) system stability following calibration, (2) increased physical eye clearance, (3) spatial filtering of high frequency noise, (4) improved lens coatings to improve see-through light transmission, (5) reduced size of lens/optics, and (6) miniaturization of electronics, if requirements go beyond simulation.

References

Rash, C.E., Kalich, M.E., van de Pol, C., and Reynolds, B.S., 2002. The Issue of Visual Correction Compatibility with Helmet Mounted Displays. Fort Rucker, AL: U.S. Army Aeromedical Research Laboratory. USAARL Report No. 2003-04.

Harding, T.H., Beasley, H.H., Martin, J.S., and Rash, C.E., 2001. Evaluation of spatial resolution in the phase II Microvision, Inc., aircrew integrated helmet system HGU-56/P scanning laser display. Fort Rucker, AL: U.S. Army Aeromedical Research Laboratory. USAARL Report No. 2002-01.

Harding, T.H., Beasley, H.H., Martin, J.S., and Rash, C.E., 2002. Evaluation of pinch correction in the phase II Microvision, Inc., aircrew integrated helmet system HGU-56/P scanning laser display. Fort Rucker, AL: U.S. Army Aeromedical Research Laboratory. USAARL Report No. 2002-013.